Vapor–Liquid Equilibrium in the System Dimethyl Ether/Methanol from 0 to 180 °C and at Pressures to 6.7 MPa

Elaine Chang,[†] Jorge C. G. Calado,[‡] and William B. Streett*

School of Chemical Engineering, Cornell University, Ithaca, New York 14853

Isothermal vapor–liquid equilibrium data have been measured for the dimethyl ether/methanol system at 10 temperatures from 0.00 to 180.00 °C, and at pressures to 6.7 MPa, by a vapor-recirculating method. Barker's method of data reduction has been used to test the thermodynamic consistency of isotherms below the critical temperature of dimethyl ether (128.8 °C). The results of the experiments have been compared with predictions of two cubic equations of state, the Redlich–Kwong and Peng–Robinson equations. With interaction parameters calculated by fitting the isotherm at 100 °C, these equations predict the liquid- and vapor-phase compositions to within about 3 mol % over most of the experimental range.

Introduction

This is the second in a series of reports on vapor–liquid equilibrium (VLE) studies of binary mixtures containing dimethyl ether (DME) and/or methanol (MeOH). VLE data for CO_2/DME have been reported (*1*), and studies of DME/H_2O are in progress. Phase equilibrium data for these systems are needed to support the development of the Mobil Process (*2*, *3*) for converting MeOH to gasoline. This catalytic process takes place in two stages: in the first stage MeOH is converted to DME, and in the second stage DME is converted to aromatic and branched paraffin hydrocarbons, predominately in the gasoline boiling range (C_4–C_{10}). The gasoline is chemically similar to that produced from crude oil (*2*). MeOH can be produced from coal, from natural gas, or from the cellulose content of plants or solid waste.

Experimental Section

The apparatus and the procedure used in this investigation are essentially the same as those used by Tsang and Streett in studies of CO_2/DME (*1*). It is a vapor-recirculating system, designed for the measurement of liquid- and vapor-phase compositions as functions of pressure at fixed temperature. Several minor modifications were made to accommodate the system DME/MeOH.

A diagram of the modified apparatus is shown in Figure 1. The equilibrium cell H, a stainless-steel vessel with a volume of 75 cm^3, is connected by a closed loop of tubing to the magnetic pump I, which circulates the vapor phase in the direction shown by the arrows. In a typcial experiment, liquid MeOH is distilled from cylinder B into the piston screw pump C, and about 25 cm^3 is injected into the system. DME is added from cylinder A to raise the pressure to the desired level, and the vapor is circulated until equilibrium is established. (The vapor pressure of DME at room temperature is about 0.5 MPa; higher pressures are obtained by controlled heating of the stainless-steel cylinder A.)

The temperature in the thermostat M is controlled to within ±0.02 °C by a Braun Model 1480 BKU proportional temperature controller T and measured by a platinum resistance thermometer R and a Mueller bridge W. A mixture of water and ethylene glycol was used as the bath fluid at temperatures up to 100 °C, and Fisher bath oil was used at higher temperatures. Pressures are measured with an uncertainty of ±0.007 MPa or ±0.5% (whichever is greater) by means of an Autoclave Model DPS digital pressure gage G, calibrated in this laboratory against a Ruska dead-weight gage.

The magnetic pump I produces a volume flow rate of 50–75 cm^3/min, sufficient to recirculate the entire vapor content of the system in about 1 min. The bubbling of vapor through the liquid provides intimate contact between the phases, and equilibrium is reached quickly, usually within 5–10 min.

After equilibrium is established, the pump is turned off, and samples of the two coexisting phases are withdrawn through the stainless-steel capillary lines J and K, into the gas chromatograph L. The chromatograph is a Hewlett-Packard Model 5840 with thermal conductivity detectors and built-in digital processor control. Samples are injected into the column in the gaseous state, at atmospheric pressure, by means of a processor-controlled sampling valve that is an integral part of the chromatograph. The manual sampling valves P and Q and all sampling lines between the thermostat and the chromatograph are heated to 150 °C to prevent condensation of the MeOH. Chromatographic separation of MeOH and DME is obtained by using helium carrier gas at 25 cm^3/min and a 6-ft long column of 100/120 mesh Porapak-R, packed in $^1/_8$-in. o.d. stainless-steel tubing. The column temperature is initially set at 125 °C, with a 30 °C/min temperature rise following the emergence of the DME peak (at about 3.5 min) to accelerate the emergence of the MeOH peak. The chromatograph was calibrated by means of mixtures of known composition prepared in this laboratory. The accuracy of the sample analyses is estimated to be ±1.0 mol %, while the overall uncertainty in the reported phase compositions is estimated to be ±1.5 mol % over most of the experimental range, increasing to about 3% for points within about 0.2 MPa from the critical line.

The MeOH used in this work, supplied by the Mallinckrodt Co., had a purity of 99.9% and a water content of less than 0.02%. It was degassed by vacuum distillation and showed no measurable impurities in a chromatographic trace analysis. The DME, from Ideal Gas Products, had an initial purity of 99.5%, the principal impurities being MeOH, CO_2, and methyl formate. It was distilled under vacuum until no measurable impurities were observed in a chromatographic trace analysis. The final purity was estimated to be 99.9% or better.

Results

Vapor and liquid compositions have been measured at 10 temperatures from 0.00 to 180.00 °C and at pressures to 6.7 MPa. The experimental results are recorded in Table I and the isotherms are plotted on pressure–composition (P–X) diagrams in Figure 2 and 3. The P–T extent of the region covered by this study is shown as the shaded area in Figure 4. In Figure 5 K values are plotted as a function of pressure ($K_i \equiv Y_i/X_i$ where Y_i is the mole fraction of component i in the vapor phase

[†] Present address: Mobil Research and Development Corp., Paulsboro, NJ 08066.
[‡] Permanent address: Instituto Superior Técnico, Lisbon 1000, Portugal.

0021-9568/82/1727-0293$01.25/0

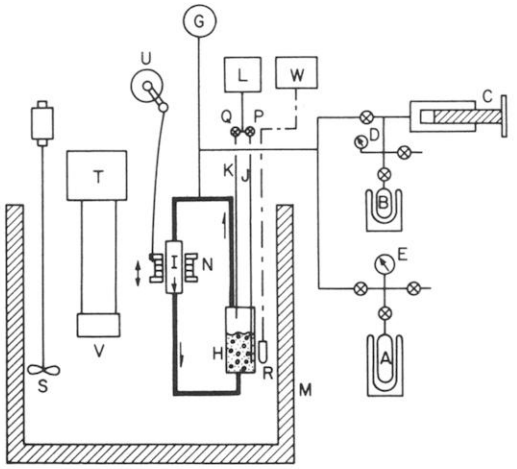

Figure 1. Diagram of apparatus: (A) stainless-steel cylinder containing dimethyl ether; (B) stainless-steel cylinder containing methanol; (C) piston screw pump; (D, E, and G) pressure gauges; (H) pressure vessel; (I) magnetically operated pump; (J and K) sampling lines; (L) gas chromatograph; (M) thermostat; (N) permanent magnets; (P and Q) sampling valves; (R) resistance thermometer; (S) stirrer; (T) proportional temperature controller; (V) circulation pump; (U) mechanical linkage; (W) Mueller bridge.

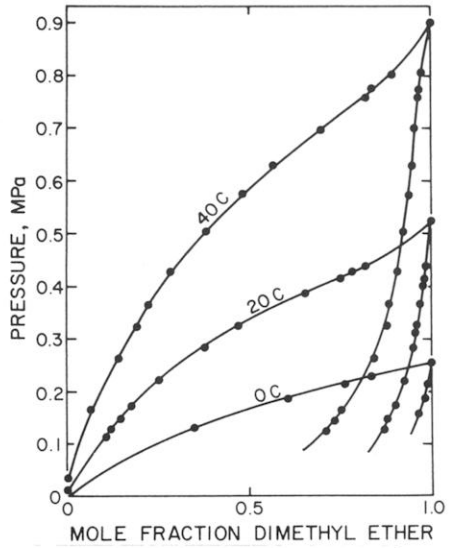

Figure 2. Experimental isotherms at 0, 20, and 40 °C.

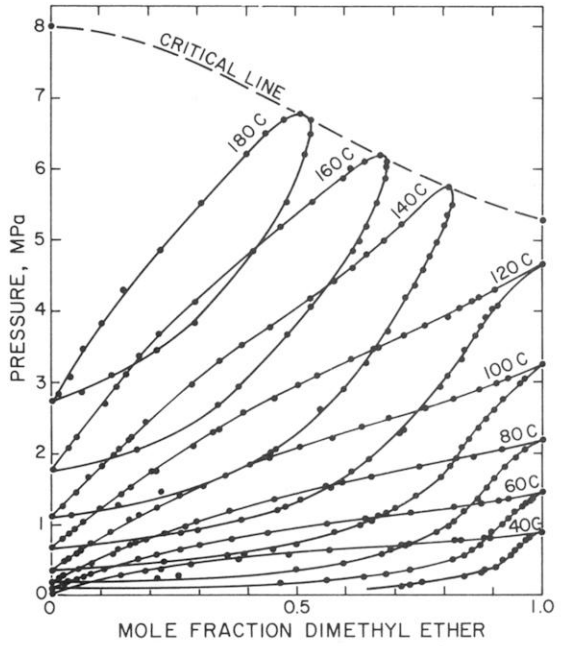

Figure 3. Experimental isotherms from 40 to 180 °C.

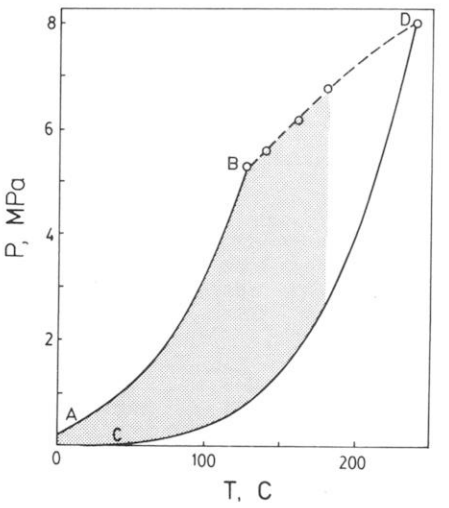

Figure 4. Pressure–temperature diagram. The shaded area is the region of $P-T$ space covered in this work. AB and CD are the vapor pressure curves of DME and MeOH, and BD is the mixture critical line.

and X_i the corresponding mole fraction in the liquid phase). Below the critical temperature of dimethyl ether, an isotherm in the K value diagram is composed of two separate branches, one for each component. Above that temperature the two branches converge at a critical point where $K = 1$, and the curve has a vertical tangent at that point. K value plots are useful as an indication of internal consistency of VLE data, because they tend to exaggerate scatter in the results; they are also useful in estimating mixture critical pressures for isotherms above the critical temperature of the more volatile component (DME). In Figures 3 and 4, that portion of the critical line between the highest experimental isotherm, 180 °C, and the methanol critical temperature, 240 °C, is only qualitative. Data for the pure-component and mixture critical points are listed in Table II.

Thermodynamic Consistency Tests

In several recent papers Van Ness and co-workers (*4–6*) examined the usefulness and limitations of several methods for testing the thermodynamic consistency of VLE data and found Barker's method (*7*) to be suitable for a wide range of applications. In applying this method to isothermal data, one fits the constants in an expression relating excess Gibbs energy to composition by a least-squares procedure that minimizes the differences between experimental and calculated pressures, using only $P-X$ data. These constants are used to calculate $P-Y$ data, via the Gibbs–Duhem equation, and the results are compared to the experimental measurement; agreement is a necessary, but not sufficient, condition for thermodynamic consistency.

In this work we have tested two expressions that relate the excess Gibbs energy G^E to composition: the three-constant Redlich–Kister equation

$$G^E = X_1X_2[a + b(X_1 - X_2) + c(X_1 - X_2)^2 + ...] \quad (1)$$

and the four-constant Margules equation

$$G^E = X_1X_2[aX_1 + bX_2 - (cX_1 + dX_2)X_1X_2] \quad (2)$$

where a, b, c, ... are constants determined by the least-squares fit. These two expressions were found to give equivalent results for DME/MeOH.

As originally developed by Barker (*7*), the consistency test is based on the assumption that the vapor phase is adequately described by a virial equation truncated after the second term.

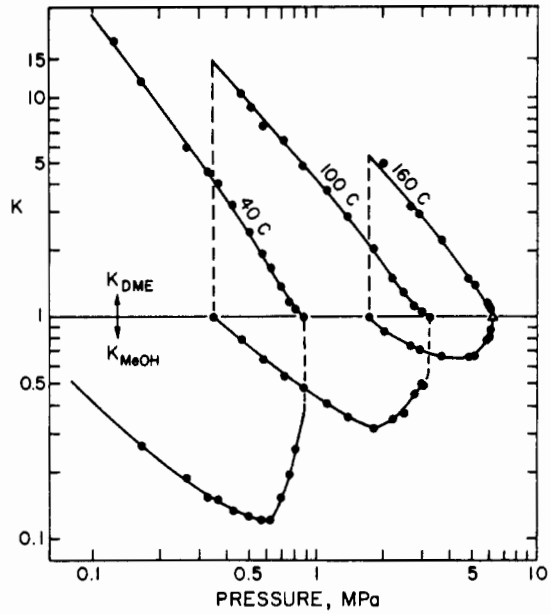

Figure 5. K value vs. pressure plots for three isotherms. The triangle on the 160 °C isotherm is the mixture critical point.

For the relatively high pressures encountered in this work, we have found it necessary to include an approximate expression for the contribution of the third virial coefficient. The total pressure is related to the activity coefficients γ_i, through

$$P = \gamma_1 X_1 P_{s_1}' + \gamma_2 X_2 P_{s_2}' \quad (3)$$

where P_{s_i}' is the "corrected vapor pressure" of component i, given by

$$P_{s_i}' = P_{s_i} \exp[(V_i^L - B_{ii}) \times (P - P_{s_i}) - P\delta_{12}(1 - Y_i)^2 - \tfrac{1}{2}C_{iii}(P^2 - P_{s_i}^2)/(RT)] \quad (4)$$

Here P_{s_i} and V_i^L are the vapor pressure and the saturated liquid volume of component i, B_{ii} and C_{iii} are the second and third pressure virial coefficients, and P is the total pressure of the mixture. δ_{12} is given by

$$\delta_{12} = 2B_{12} - B_{11} - B_{22} \quad (5)$$

where B_{12} is the second cross virial coefficient. The term involving C_{iii} in eq 4 is an approximation, based on the assumption of linear dependence of C on composition for the mixture (*8*). Values for the second virial coefficients of the pure components and the mixture were estimated by using the method described by Tsonopoulos (*9*). Third virial coefficients for DME were estimated from the corresponding states correlation of Chueh and Prausnitz (*10*), and those for the MeOH were estimated by extrapolation of the experimental measurements of Keil and McLauren (*11*) on a plot of ln (C) against T. Vapor pressures and saturated liquid volumes were taken from the data of Zubarev et al. (*12*) for MeOH and of Cardoso and Bruno (*13*) for DME. The physical properties and virial coefficients are summarized Table III.

Detailed instructions for the implementation of Barker's method can be found in his original paper (*7*). Modern nonlinear least-squares subroutines, available from subroutine libraries in most large computing centers, are easier to use and more reliable than the numerical procedures outlined by Barker. The constants for eq 1, obtained by least-squares fitting of the P–X data, are listed in Table IV.

Figure 6 shows a comparison of the experimental, fitted, and predicted P–X–Y data for four isotherms. The pressure deviations scatter randomly about zero, and the differences between experimental and predicted vapor compositions are about 1.0–1.5%, which is within the combined uncertainties in

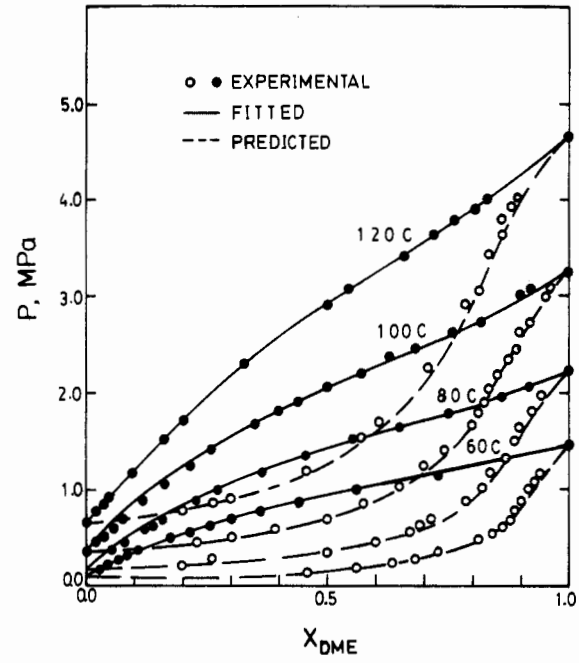

Figure 6. Comparison of experimental, fitted, and predicted data from the thermodynamic consistency test using Barker's method (*7*).

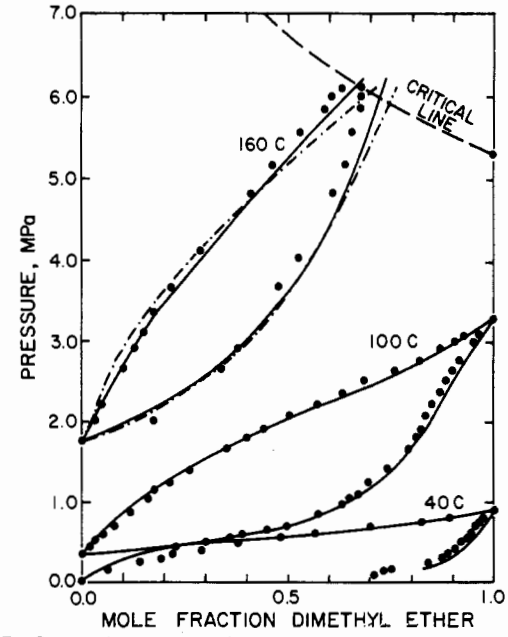

Figure 7. Comparison of experimental results with the predictions of the Peng–Robinson and Redlich–Kwong equations of state: (●) experiment; (—) Peng–Robinson equation; (– · –) Redlich–Kwong equation. At 40 and 100 °C the predictions of the two equations are indistinguishable.

the experimental liquid and vapor compositions. We therefore conclude that the thermodynamic consistency test is satisfied.

If the third virial coefficient is omitted from eq 4, the predicted and observed vapor compositions agree at pressures up to about 1.5 MPa but differ by as much as 5 mol % at higher pressures. At the lowest three isotherms, 0, 20 and 40 °C, the vapor pressure of MeOH is small compared to the total pressure of the mixture over most of the range of compositions. Van Ness (*4*) has pointed out that under these conditions a meaningful thermodynamic consistency test is possible only if very careful measurements of pure-component vapor pressures are made with the same apparatus used in studying the mixtures. (This is due to the direct dependence of the corrected vapor pressure, P_s', on the saturation vapor pressure, P_s, in eq 4.) In this work we were unable to measure the saturation

Table I. Experimental Vapor-Liquid Compositions for DME/MeOH[a]

P, MPa	X_1	Y_1	P, MPa	X_1	Y_1
		T = 0.00 °C			
0.004	0.000	0.000	0.214	0.761	0.990
0.131	0.346		0.228	0.834	
0.159		0.966	0.255	1.000	1.000
0.186	0.606	0.983			
		T = 20.00 °C			
0.013	0.000	0.000	0.324	0.468	0.959
0.114	0.105		0.365		0.966
0.128	0.120	0.869	0.386	0.652	
0.148	0.145	0.879	0.414	0.749	0.977
0.172	0.175	0.900	0.427	0.784	
0.221	0.251	0.924	0.438	0.821	0.983
0.283	0.378	0.948	0.521	1.000	1.000
0.310		0.955			
		T = 40.00 °C			
0.036	0.000	0.000	0.503	0.380	0.922
0.124		0.711	0.572	0.483	0.937
0.145		0.733	0.627	0.565	0.946
0.165	0.064	0.753	0.696	0.701	0.954
0.262	0.141	0.840	0.758	0.821	0.965
0.324	0.193	0.876	0.772	0.834	0.967
0.365	0.222	0.883	0.800	0.893	0.973
0.427	0.283	0.905	0.900	1.000	1.000
		T = 60.00 °C			
0.086	0.000	0.000	0.779	0.367	0.882
0.159	0.027	0.456	0.869	0.440	0.897
0.165	0.030	0.466	0.993	0.560	0.918
0.214	0.050	0.560	1.069	0.639	0.931
0.248	0.064	0.635	1.165	0.732	0.943
0.290	0.080	0.680	1.241	0.820	0.960
0.345	0.105	0.730	1.282	0.874	0.966
0.490	0.175	0.816	1.324	0.910	0.975
0.552	0.214	0.841	1.344	0.932	0.981
0.627	0.262	0.856	1.461	1.000	1.000
0.683	0.300	0.875			
		T = 80.00 °C			
0.182	0.000	0.000	0.972	0.270	0.808
0.221	0.014	0.214	1.027	0.294	0.818
0.269	0.021	0.258	1.172	0.363	0.839
0.352	0.053	0.498	1.344	0.454	0.869
0.434	0.081	0.594	1.517	0.557	0.888
0.565	0.123	0.671	1.655	0.650	0.902
0.621	0.133	0.690	1.800	0.749	0.924
0.689	0.158	0.713	1.944	0.860	0.945
0.717	0.167	0.726	2.041	0.917	0.963
0.876	0.229	0.784	2.243	1.000	1.000
		T = 100.00 °C			
0.353	0.000	0.000	1.531	0.308	
0.462	0.022	0.228	1.669	0.352	0.794
0.517	0.033	0.300	1.820	0.402	0.812
0.552		0.360	1.924	0.440	0.823
0.579	0.052	0.391	2.075	0.506	0.835
0.614	0.057		2.206	0.571	0.852
0.648		0.451	2.351	0.632	0.870
0.717	0.078	0.498	2.482	0.686	0.885
0.869	0.119	0.576	2.620	0.762	0.900
0.979		0.630	2.758	0.820	0.919
1.048	0.162	0.652	2.896	0.871	
1.117	0.177	0.664	2.979	0.906	0.953
1.145		0.679	3.047	0.927	0.964
1.241	0.216	0.697	3.256	1.000	1.000
1.393	0.261	0.740			
		T = 120.00 °C			
0.640	0.000	0.000	2.317	0.340	0.716
0.779	0.022	0.190	2.551	0.388	
0.862	0.035	0.263	2.744	0.454	
0.910	0.045	0.297	2.930	0.500	0.791
1.007	0.062		3.082	0.541	0.806
1.048		0.385	3.296	0.609	
1.193	0.097	0.459	3.447	0.656	0.836
1.331		0.506	3.647	0.718	0.862
1.420	0.144		3.778	0.760	0.873
1.503	0.161	0.568	3.909	0.807	0.881
1.572		0.592	4.020	0.830	0.897

Table I (*Continued*)

P, MPa	X_1	Y_1	P, MPa	X_1	Y_1
1.724	0.202	0.609	4.137	0.857	
1.903		0.645	4.192	0.870	
2.075	0.285		4.289	0.906	
2.275	0.327	0.710	4.663	1.000	1.000
			T = 140.00 °C		
1.083	0.000	0.000	3.468		0.664
1.117	0.004	0.041	3.503	0.387	
1.241	0.022	0.133	3.716		0.686
1.441	0.049	0.221	3.765	0.443	
1.627	0.074		4.158	0.527	
1.813	0.103		4.185		0.722
1.924		0.434	4.364		0.743
1.958	0.128		4.399	0.575	
1.993		0.445	4.578	0.614	0.758
2.027	0.136	0.455	4.771		0.770
2.172	0.156		4.792	0.642	
2.193	0.160		4.957		0.786
2.427	0.191		4.978	0.677	
2.882		0.593	5.205	0.717	0.799
2.910	0.285		5.330		0.807
3.247		0.642	5.481		0.817
3.289	0.342		(5.743)[b]	(0.808)	(0.808)
			T = 160.00 °C		
1.749	0.000	0.000	4.109	0.290	
2.034	0.035	0.174	4.826	0.412	0.614
2.206	0.050		5.171	0.463	0.641
2.654	0.107	0.338	5.516	0.532	0.661
2.910	0.130	0.380	5.854	0.593	0.680
3.096	0.152		5.998	0.609	0.682
3.351	0.176		6.081	0.637	0.684
3.654	0.217	0.479	(6.171)[b]	(0.670)	(0.670)
4.033		0.528			
			T = 180.00 °C		
2.703	0.000	0.000	4.826	0.221	
2.827	0.015	0.062	5.516	0.304	0.478
3.068	0.038	0.122	6.205	0.396	0.517
3.447	0.065	0.221	6.481	0.435	0.525
3.820	0.101	0.290	6.674	0.474	0.527
4.289	0.144		(6.750)[b]	(0.505)	(0.505)

[a] X_1 is the mole fraction of DME in the liquid and Y_1 is the mole fraction of DME in the vapor. Pure-component vapor pressures are from the literature (*12, 13*). [b] Mixture critical points have been estimated by extrapolation of experimental measurements.

Table II. Vapor-Liquid Critical Line for DME/MeOH

temp, °C	press., MPa	DME mole fraction	temp, °C	press., MPa	DME mole fraction
240.00[a]	8.103	0.000	140.00	5.743	0.808
180.00	6.750	0.505	128.8[b]	5.32	1.000
160.00	6.171	0.670			

[a] Critical data from Zubarev et al. (*12*). [b] Critical data from Cardoso and Bruno (*13*).

vapor pressures of MeOH at low temperatures with high precision, and we have used values from the literature (*12*, *13*). The use of these values in thermodynamic consistency tests leads to differences in predicted and experimental vapor compositions of 3–5 mol %; however, these differences are reduced to 1.0–1.5% if the saturation vapor pressures are adjusted by as little as 0.006 MPa, which is within the precision of our pressure measurement for the mixture.

Equation of State Calculations

The experimental data have been compared with the predictions of two equations of state, the Redlich–Kwong (RK) equation (*14*) and the Peng–Robinson (PR) equation (*15*):

RK equation

$$P = \frac{RT}{V - b} - \frac{a}{T^{1/2}V(V + b)} \tag{6}$$

PR equation

$$P = \frac{RT}{V - b} - \frac{a(T)}{V(V + b) + b(V - b)} \tag{7}$$

Table III. Physical Properties of DME (Component 1) and MeOH (Component 2)[a]

T, °C	P_{s_1}, MPa	P_{s_2}, MPa	V_1, cm³/mol	V_2, cm³/mol	B_{11}, cm³/mol	B_{22}, cm³/mol	B_{12}, cm³/mol	C_{111}, cm³/(MPa mol)	C_{222}, cm³/(MPa mol)
40.00	0.900	0.036	73.30	41.49	−422	−1513	−389	−63	−3100
60.00	1.461	0.086	77.66	42.58	−358	−1020	−319	−41	−1550
80.00	2.243	0.182	83.38	43.80	−309	−730	−269	−27	−740
100.00	3.256	0.353	93.64	45.18	−269	−550	−231	−18	−400
120.00	4.663	0.640	114.8	46.78	−237	−434	−200	−12	−210

[a] Pure-component data for MeOH from Zubarev et al. (*12*) and for DME from Cardoso and Bruno (*13*).

Table IV. Constants for the Redlich-Kister Equation (Eq 1) for Five Isotherms

temp, °C	a	b	c
40.00	1.0229	0.0546	0.0055
60.00	0.9338	0.0687	0.0292
80.00	0.8713	0.0428	−0.0762
100.00	0.8533	0.0428	−0.0664
120.00	0.8248	0.0355	−0.0607

The parameters a and b are concentration dependent, and the mixing rules for binary mixtures are

$$a_m = a_{11}X_1^2 + 2a_{12}X_1X_2 + a_{22}X_2^2$$

$$b_m = b_{11}X_1 + b_{22}X_2 \quad (8)$$

where a_{12} is given by

$$a_{12} = (1 - k_{12})(a_{11}a_{22})^{1/2}$$

The parameter k_{12} represents the deviation of a_{12} from the classical geometric mean assumption.

For the Redlich–Kwong equation, the values of a_{11}, b_{11}, a_{22}, and b_{22} are evaluated from critical or $P-V-T$ data of the pure components, as recommended by Joffe and Zudkevitch (*16*, *17*). For the PR equation, the temperature dependence of the constant a is given by an expression based on the Pitzer acentric factor (*15*).

The parameter k_{12} is adjusted by trial and error to produce agreement between the chemical potentials or fugacities in the saturated vapor and liquid phases, a constraint of binary equilibrium. This fitting procedure is applied to an isotherm near the middle of the experimental range (100 °C in this case). k_{12} is assumed to be independent of temperature, pressure, and composition. The calculated interaction parameters for DME/MeOH are $k_{12} = 0.0252$ for the PR equation and $k_{12} = -0.0065$ for the RK equation.

Tests of the equation of state predictions have been made by comparing experimental and predicted isotherms near the extremes of the experimental range of temperatures. The comparisons are summarized in Figure 7, which shows the fitted isotherm, 100 °C, together with isotherms at 40 and 160 °C. At 40 and 100 °C the predictions of the PR and RK equations are indistinguishable. At 160 °C, neither equation agrees well with experiment over the entire range of pressures; however, the PR equation is marginally better.

Literature Cited

(1) Tsang, C. Y.; Streett, W. B. *J. Chem. Eng. Data* **1981**, *26*, 155.
(2) Chang, C. D.; Silvestri, A. J. *J. Catal.* **1977**, *47*, 249.
(3) Harney, B. M.; Mills, A. G. *Hydrocarbon Process.* **1980**, *59*, 67.
(4) Van Ness, H. C.; Byer, S. M.; Gibbs, R. E. *AIChE J.* **1973**, *19*, 236.
(5) Byer, S. M.; Gibbs, R. E.; Van Ness, H. C. *AIChE J.* **1973**, *19*, 245.
(6) Abbott, M. M.; Van Ness, H. C., *AIChE J.* **1975**, *21*, 62.
(7) Barker, J. A. *Aust. J. Chem.* **1953**, *6*, 207.
(8) Calado, J. C. G. *Têcnica* **1972**, *34*, 237.
(9) Tsonopoulos, C. *AIChE J.* **1974**, *20*, 263.
(10) Chueh, P. L.; Prausnitz, J. M. *AIChE J.* **1967**, *13*, 896.
(11) Kell, G. S.; McLauren, G. E. J. *J. Chem. Phys.* **1969**, *51*, 4345.
(12) Zubarev, V. N.; Prusakov, P. G.; Sergeeva, L. V., data obtained from IUPAC Thermodynamic Table Project Center, Imperial College of Science, London, 1980.
(13) Cardoso, E.; Bruno, A. *J. Chem. Phys.* **1923**, *20*, 347.
(14) Redlich, O.; Kwong, J. W. S. *Chem. Rev.* **1949**, *44*, 233.
(15) Peng, D. Y.; Robinson, D. B. *Ind. Eng. Chem. Fundam.* **1976**, *15*, 159.
(16) Joffe, J.; Zudkevitch, D. *AIChE J.* **1970**, *16*, 112.
(17) Joffe, J.; Schroeder, G. M.; Zudkevitch, D. *AIChE J.* **1970**, *16*, 496.

Received for review July 24, 1981. Accepted February 8, 1982. Acknowledgment is made to the donors of the Petroleum Research Fund, administered by the American Chemical Society, for partial support of this work. This work was also supported, in part, by a grant from the Mobil Research and Development Corp. and by grants CPE 78-23537 and 79-09166 from the National Science Foundation.

Partial Miscibility Behavior of the Ternary Systems Methane–Propane–*n*-Octane, Methane–*n*-Butane–*n*-Octane, and Methane–Carbon Dioxide–*n*-Octane

John D. Hottovy, James P. Kohn,* and Kraemer D. Luks†

Department of Chemical Engineering, University of Notre Dame, Notre Dame, Indiana 46556

The phase behavior of three ternary systems (methane–propane–*n*-octane, methane–*n*-butane–*n*-octane, methane–carbon dioxide–*n*-octane) was studied in their regions of L_1–L_2–V immiscibility. Liquid-phase composition and molar volume data for both liquid phases are presented as a function of temperature and pressure in the three-phase region. The boundaries of the three-phase regions, loci of K points (L_1–L_2 = V), LCST points (L_1 = L_2–V), and Q points (S–L_1–L_2–V) are detailed. A detailed study of the immiscibility behavior of the binary system carbon dioxide–*n*-octane is also presented.

Introduction

We have undertaken an extensive study of liquid–liquid–vapor (L_1–L_2–V) phenomena in liquefied natural gas (LNG) systems. In an earlier paper (*1*), we reported the L_1–L_2–V immiscibility region, including its K-point (L_1–L_2 = V), LCST (L_1 = L_2–V), and Q-point (S–L_1–L_2–V) boundaries, for the ternary system methane–ethane–*n*-octane. This system does not exhibit immiscibility in any of its binary pairs. Although immiscibility has been reported in binary systems of methane–*n*-hexane (*2*) and methane–*n*-heptane (*3*), solutes such as *n*-octane and higher normal paraffins crystallize as temperature decreases before any immiscibility occurs (*4*). On the other hand, with ethane as solvent, solutes beginning with *n*-C_{19} and higher *n*-paraffins demonstrate L_1–L_2–V behavior (*5*–*7*). Apparently, the addition of modest amounts of ethane to methane creates a solvent mixture capable of exhibiting immiscibility with *n*-octane.

In this present paper, we present results on three new ternary systems which exhibit immiscibility due to the addition of a heavier solvent species to the binary system methane–*n*-octane. The additives for the three new ternary systems are propane, *n*-butane, and carbon dioxide, respectively. With propane, only very long-chain hydrocarbons (*n*-C_{37} and higher *n*-paraffins) demonstrate binary L_1–L_2–V behavior (*6*). Carbon

† Recent address: Department of Chemical Engineering, University of Tulsa, Tulsa, Ok 74104.

0021-9568/82/1727-0298$01.25/0